Editors' Suggestion | Featured in Physics

Purely Electronic Chirality without Structural Chirality

Takayuki Ishitobi[1,2] and Kazumasa Hattori[2]
[1]Advanced Science Research Center, Japan Atomic Energy Agency, Tokai, Ibaraki 319-1195, Japan
[2]Department of Physics, Tokyo Metropolitan University, 1-1, Minami-osawa, Hachioji, Tokyo 192-0397, Japan

(Received 15 February 2025; revised 5 November 2025; accepted 3 December 2025; published 4 February 2026)

We introduce the concept of purely electronic chirality (PEC), which arises in the absence of structural chirality. In condensed matter physics and chemistry, chirality has conventionally been understood as a mirror-image asymmetry in crystal or molecular structures. We demonstrate that certain electronic orders exhibit chirality-related properties without atomic displacement. Specifically, we investigate quadrupole orders to realize such purely electronic chirality with handedness that can be tuned by magnetic fields. As a representative example, we analyze a model featuring 120° antiferro quadrupole orders on a distorted kagome lattice, predicting various chirality-related responses in the nonmagnetic ordered phase of URhSn. Furthermore, as a phonon analog, chiral phonons can emerge in achiral crystals through coupling with the PEC order. Our results provide a distinct origin of chirality and a fundamental basis for exploring the interplay between electronic and structural chirality.

DOI: 10.1103/dc1q-xzbd

Introduction—Chirality, grounded in the asymmetry between an object and its mirror image, manifests across diverse fields of natural science [1]. Since Pasteur's seminal discovery of the connection between optical activity and molecular chirality [2], this concept has evolved to encompass phenomena such as parity symmetry breaking in particle physics [3,4] and the double-helix structure of DNA [5,6]. In materials science, chirality is typically understood as the mirror asymmetry of atomic positions, whereas in particle physics, it is defined through the internal degrees of freedom in elementary particles. This raises the fundamental question: can the concept of chirality in materials science exist independently of mirror asymmetry in atomic positions?

Recently, it has been shown that the order parameter of chirality is the electric toroidal monopole (ETM) [7,8], a time-reversal even pseudoscalar [9,10] in electronic degrees of freedom. Since then, the ETM has attracted significant attention, linking it to the chirality of Dirac electrons [11], possible antiferroic ordering of the atomic chirality [12], and first-principle evaluation of ETM [13,14]. However, despite these advancements, the source of orderings of the electronic chirality has been considered due to the structural origin.

In this Letter, we show that the electronic chirality can emerge solely from electronic orderings *without* structural chirality. This phenomenon occurs in achiral systems through the chiral symmetry breaking while preserving the original achiral structure. We call it *purely* electronic chirality (PEC). We outline a way to construct the chirality from electric quadrupole moments of electrons, as the electric quadrupole moments are active in various systems with orbital degrees of freedom.

Construction of purely electronic chirality—The most straightforward approach to constructing the ETM G_0 is to take the inner product of polar and axial vectors, $G_0 \propto \boldsymbol{G}\cdot\boldsymbol{Q}$, where $\boldsymbol{Q}=(Q_x,Q_y,Q_z)$ represents the electric dipole moment, and $\boldsymbol{G}=(G_x,G_y,G_z)$ denotes the electric toroidal dipole moment. In the following, we denote time-reversal even polar (axial) tensors as Q's (G's) [15]. To construct G_0 via the relation $G_0 \propto \boldsymbol{G}\cdot\boldsymbol{Q}$, both $\boldsymbol{G}$ and $\boldsymbol{Q}$ must be present as microscopic degrees of freedom, whereas they need not be finite in the bulk. We note that rotational symmetry prohibits finite bulk $\boldsymbol{G}$ and $\boldsymbol{Q}$ perpendicular to the rotational axis, while it imposes no restrictions on the scalar G_0. A quantum mechanical expression of the axial vector $\boldsymbol{G}$ is $\boldsymbol{G}=\boldsymbol{l}\times\boldsymbol{\sigma}$, where $\boldsymbol{l}$ and $\boldsymbol{\sigma}$ are the orbital and spin angular momentum operators for the electron, respectively [15]. A key observation is that certain quadrupole moments $Q_{\mu\nu}=Q_{\nu\mu}$ ($\mu,\nu=x,y,z$) and $\boldsymbol{G}$ are hybridized by uniaxial crystalline electric fields $O_{20}\propto 3l_z^2-l(l+1)$ in two-dimensional systems. This hybridization enables the realization of PEC through simple quadrupole orders in layered systems. Consider the coupling between the spin-orbital hybridized electric quadrupole $Q^{\mathrm{hyb}}_{yz(zx)}\propto l_z\sigma_{y(x)}+l_{y(x)}\sigma_z$ and the electric toroidal dipole $G_{x(y)}\propto l_z\sigma_{y(x)}-l_{y(x)}\sigma_z$ moments: a straightforward calculation shows $\mathrm{Tr}[Q^{\mathrm{hyb}}_{yz(zx)}G_{x(y)}O_{20}]\neq 0$, while $\mathrm{Tr}[Q^{\mathrm{hyb}}_{yz(zx)}G_{x(y)}]=0$, where Tr denotes summation over a given rotationally symmetric multiplet with the orbital angular momentum l and the spin-$\frac{1}{2}$ manifold.

Published by the American Physical Society under the terms of the Creative Commons Attribution 4.0 International license. Further distribution of this work must maintain attribution to the author(s) and the published article's title, journal citation, and DOI.

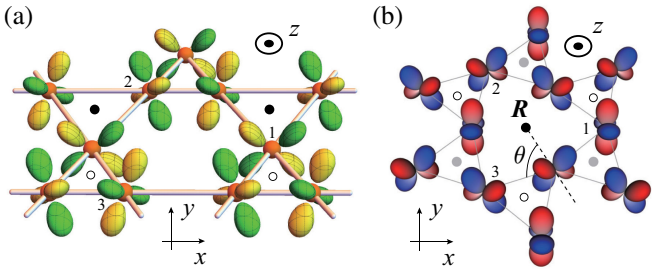


FIG. 1. Examples of purely electronic chirality in achiral crystals due to quadrupole moments. (a) Breathing kagome and (b) distorted kagome structures. The sublattice labels are indicated as $n = 1, 2, 3$. Circles indicate threefold rotation axes. The filled, open, and gray circles represent inequivalent axes. In (b), the position of the unit cell is taken at the center of the distorted hexagon and denoted as $\boldsymbol{R}$. θ is the distortion angle parameter; $\theta = 60°$ for regular kagome structure.

We now describe our setup and present examples of PEC. To realize PEC, the order parameter must not involve any polar vector associated with atomic displacements, such as a local electric dipole moment or an induced local electric field. Equivalently, the equilibrium atomic positions $\boldsymbol{r}_n (n = 1, 2, \ldots)$ inside the unit cell remain unchanged with $\boldsymbol{r}_n$'s being the positions of atoms where the electric quadrupoles are defined.

To illustrate these concepts, we show simple uniform ($\boldsymbol{q} = \boldsymbol{0}$) orders in two-dimensional kagome type structures in Fig. 1: (a) breathing and (b) distorted kagome structures. Here, the "breathing" and "distorted" are the key features enabling PEC, which allow finite polar vectors, e.g., at the position $\boldsymbol{r}_1$, $\sim Q_y$ in (a) and Q_x in (b). The twofold rotational symmetry along the y- and x-axes ensures that the atomic positions remain unchanged for (a) and (b), respectively, thereby ensuring the PEC feature. Additional examples, including quadrupole orders in breathing square, breathing honeycomb, and tetragonal diamond lattices, and several cubic examples, are provided in the Supplemental Material (SM) [16–22]. In these examples, PEC arises under a sufficient condition; a polar vector component originating from the crystal structure (e.g., Q_x) coexists with an ordered quadrupole component involving different coordinates (Q_{yz}) that hybridizes with the axial vector (G_x). This coupling, $G_0 \propto \boldsymbol{Q} \cdot \boldsymbol{G}$, produces chirality without inducing any additional polar vector, thereby preserving the crystal structure.

Chirality in distorted kagome systems—We now discuss the PEC orders in more detail, taking the distorted kagome system [Fig. 1(b)] as a representative example. We demonstrate that a simple 120° order of the electric quadrupole $\{Q_{yz}, Q_{xz}\}$ is a PEC order. This state has a realistic manifestation and excels in distinguishing the sign of chirality (left and right handedness). The chirality couples to the magnetic field, rendering the positive and negative chirality domains inequivalent. As an ideal platform to explore the electronic chirality, we propose a promising candidate, URhSn [23–29], later in this Letter.

We introduce the chirality order parameter consisting of three quadrupole moments of the localized electrons in a unit cell at $\boldsymbol{R}$ of the distorted kagome structure. See Fig. 1(b). We label the three sublattices by $n = 1, 2, 3$ and denote their positions $\boldsymbol{r}_n \equiv \ell\{\cos[2(n-1)\pi/3], \sin[2(n-1)\pi/3], 0\}$ with $\ell > 0$ being a distance of the atomic position from the center of the distorted hexagon at $\boldsymbol{R}$. We express the local degrees of freedom at $\boldsymbol{R}$ as a direct product of the quadrupole and sublattice parts. The quadrupole moments are written as $\{Q^{\boldsymbol{R}}_{yz}, Q^{\boldsymbol{R}}_{xz}\}$. The local electric dipoles for the sublattice degrees of freedom are defined as $\hat{Q}_\mu = \sum_{n=1,2,3} (\hat{\boldsymbol{r}}_n)_\mu \hat{P}_n$ with $\hat{\boldsymbol{r}}_n = \boldsymbol{r}_n/|\boldsymbol{r}_n|$ and $\hat{P}_n$ being the projection operator to the states at the nth sublattice. The chirality at the unit cell $\boldsymbol{R}$ is defined as

$$\mathcal{C}_{\boldsymbol{R}} \equiv \sum_{\mu,\nu=x,y} \epsilon_{\mu\nu z} \hat{Q}_\mu Q^{\boldsymbol{R}}_{\nu z}, \tag{1}$$

where $\epsilon_{\mu\nu\lambda}$ is the totally antisymmetric tensor. $\mathcal{C}_{\boldsymbol{R}}$ is a rank-2 axial tensor, electric toroidal quadrupole moment G_{zz}, and transforms as G_0 in the presence of uniaxial anisotropy Q_{zz}: $\mathrm{Tr}[G_0 G_{zz} Q_{zz}] \neq 0$.

The chirality generated by $Q^{\boldsymbol{R}}_{\mu z}$ can couple with conduction electrons in metallic systems. Consider a two-orbital itinerant model with $\{p_x, p_y\}$, $\{d_{zx}, d_{yz}\}$, or $\{d_{x^2-y^2}, d_{xy}\}$ orbitals under the PEC order in distorted kagome structure. Since the orbital angular momentum of the conduction electrons $l^{\boldsymbol{R}}_{x,y}$ is not active in the two-orbital model, the active electric quadrupoles at $\boldsymbol{R}$ are $l^{\boldsymbol{R}}_z \sigma^{\boldsymbol{R}}_{y(x)}$, which couple with the local electric quadrupole $Q^{\boldsymbol{R}}_{yz(xz)}$. Here, $l^{\boldsymbol{R}}_z (\sigma^{\boldsymbol{R}}_\mu)$ is the orbital (spin) angular momentum at $\boldsymbol{R}$. Then, the local quadrupole-quadrupole coupling in the presence of $\boldsymbol{q} = \boldsymbol{0}$ chirality order $\langle \mathcal{C}_{\boldsymbol{R}} \rangle = \bar{\mathcal{C}}$ is given by

$$\sum_n \sum_{\mu=x,y} \hat{P}_n \langle Q^{\boldsymbol{R}}_{\mu z} \rangle \sigma^{\boldsymbol{R}}_\mu l^{\boldsymbol{R}}_z = g(\hat{Q}_x \sigma^{\boldsymbol{R}}_y - \hat{Q}_y \sigma^{\boldsymbol{R}}_x) l^{\boldsymbol{R}}_z \equiv V_{\boldsymbol{R}}, \tag{2}$$

where g is a phenomenological coupling constant proportional to $\bar{\mathcal{C}}$, and $\hat{P}_n$ now operates also on the conduction electron Hilbert space. Equation (2) gives rise to phenomena characteristic of chirality even in the absence of structural changes, as discussed below.

To illustrate such phenomena, we consider a toy model involving the spin-independent nearest-neighbor (NN) hopping H_0 and $V_{\boldsymbol{R}}$, which exhibits spin-splitting dispersion characteristic of chiral systems. The Hamiltonian is given by $H = H_0 + \sum_{\boldsymbol{R}} (V_{\boldsymbol{R}} - \mu_c N_{\boldsymbol{R}})$, where $N_{\boldsymbol{R}}$ is the number operator at $\boldsymbol{R}$, and μ_c is the chemical potential. H_0 includes the σ- and π-bonds hoppings t_σ and t_π, respectively. In the Fourier space, $H = \sum_{\boldsymbol{k}} H_{\boldsymbol{k}}$, and the Bloch Hamiltonian $H_{\boldsymbol{k}}$ has twelve eigenvalues, $\epsilon_{\boldsymbol{k}}$'s, at each wave number $\boldsymbol{k} = (k_x, k_y)$. Detail of the model is shown in the SM [16]. Figures 2(a) and 2(b) show the single-particle energy $\epsilon_{\boldsymbol{k}}$ and Fermi surfaces (FSs). In Fig. 2(b), one can clearly see the

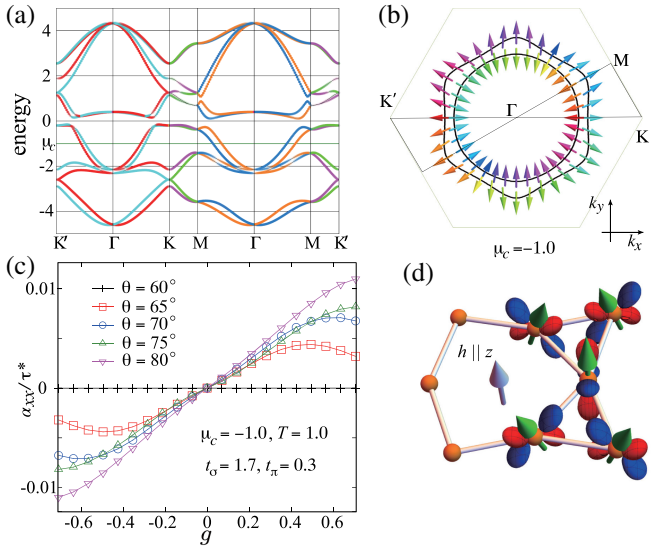


FIG. 2. (a) Dispersion $\epsilon_{\boldsymbol{k}}$ along the path K′-Γ-K-M-Γ-M-K′ for $k_x k_y \geq 0$ indicated by the line in (b) for $g = 1/\sqrt{2}$, $t_\sigma = 1.7$, $t_\pi = 0.3$, and $\theta = 75°$ with the other parameters being indicated in (c). Color represents the direction of spin $\boldsymbol{\sigma}_{\boldsymbol{k}}$ for the Bloch state on the xy plane as illustrated in (b). (b) Fermi surfaces for $\mu_c = -1$. $\boldsymbol{\sigma}_{\boldsymbol{k}}$'s are on the xy plane and indicated by arrows. (c) $\alpha_{xx}(=\alpha_{yy})$ as a function of g for $\mu_c = -1$, $T = 1.0$ and for several values of distortion angle θ. $\theta = 60°$ corresponds to the regular kagome. (d) A schematic configuration of quadrupole and magnetic moments under magnetic fields along the z direction inside the chiral phase or the FM state with the chiral quadrupole order. Green arrows are the magnetic moments that tilt toward the quadrupole principal axis, and this induces a finite scalar spin chirality for the triangular plaque.

Bloch band spin $\boldsymbol{\sigma}_{\boldsymbol{k}} \parallel \boldsymbol{k}$ due to the (anti-) hedgehog-type spin-splitting $\sim \boldsymbol{k} \cdot \boldsymbol{\sigma}$ on the FSs, even in the absence of structural chirality.

Let us consider the microscopic origin of the hedgehog-type spin splitting. Even if $H_{\boldsymbol{k}}$ does not explicitly contain the $\boldsymbol{k} \cdot \boldsymbol{\sigma}$ terms, one can investigate whether such terms exist in the eigenvalues $\epsilon_{\boldsymbol{k}}$ by examining the pth power of the Hamiltonian $H^p_{\boldsymbol{k}} (p \geq 2)$ expressed in the symmetry-adapted basis [30]. The technique has been applied to elucidate microscopic mechanisms underlying various phenomena such as anomalous Hall effects and spin splittings in the Bloch states [31–33]. As the chiral order parameter $\bar{\mathcal{C}}$ must be essential for the emergence of the hedgehog-type spin-momentum locking, we examine the symmetric product of $V_{\boldsymbol{R}}$ and $\boldsymbol{k} \cdot \boldsymbol{\sigma}$ and obtain

$$\{(\hat{Q}_x \sigma_y - \hat{Q}_y \sigma_x) l_z, \boldsymbol{k} \cdot \boldsymbol{\sigma}\} = 2(k_x \hat{Q}_y - k_y \hat{Q}_x) l_z. \quad (3)$$

This expression represents a sublattice-dependent orbital Rashba coupling [34] and should appear in $H^p_{\boldsymbol{k}}$ for generating the spin splittings. We note that related orbital-momentum couplings have recently been observed in chiral crystals [35], highlighting their manifestation in real materials. In fact, the product of the real part ($\propto k^0$) and imaginary part $\propto k^1$ of the NN hoppings includes Eq. (3). See the SM [16] for the details. This means that the hedgehog-type spin splitting in $\epsilon_{\boldsymbol{k}}$ originates from $H^3_{\boldsymbol{k}}$ and is proportional to $\bar{\mathcal{C}}$.

The spin-momentum locking leads to a finite current-induced magnetization commonly known as the Edelstein effect [36]. Figure 2(c) shows the magnetoelectric coefficient $\alpha_{\mu\nu}$, where the distortion is controlled by the angle parameter θ defined in Fig. 1(b). $\alpha_{\mu\nu}$ is analyzed by the conventional Boltzmann transport theory $\alpha_{\mu\nu} = -\tau^* \sum_{\boldsymbol{k}} (\boldsymbol{\sigma}_{\boldsymbol{k}})_\mu (\partial \epsilon_{\boldsymbol{k}} / \partial k_\nu) (\partial n_{\boldsymbol{k}} / \partial \epsilon_{\boldsymbol{k}})$, where the summation runs over all the bands; $n_{\boldsymbol{k}}$ is the Fermi distribution for $\epsilon_{\boldsymbol{k}}$; and τ^* is the phenomenological relaxation time. α's vanish for the regular kagome system ($\theta = 60°$). As mentioned above, the spin-momentum locking $\boldsymbol{k} \cdot \boldsymbol{\sigma}$ leads to the longitudinal response $\alpha_{xx} = \alpha_{yy} \neq 0$ and $\alpha_{xy} = \alpha_{yz} = 0$. Note that this effect occurs without the structural chirality of crystal. We also note that a recent study, involving one of the present authors, has examined the effects of chirality fluctuations on the α coefficients [37].

Chirality-induced couplings—To obtain the qualitative understanding of the electronic chirality order, we perform a Landau theoretical analysis for the uniform $\boldsymbol{q} = \boldsymbol{0}$ chirality order with $\langle \mathcal{C}_{\boldsymbol{R}} \rangle = \bar{\mathcal{C}}$. In contrast to the structural degrees of freedom, the electronic degrees of freedom can couple strongly to magnetic degrees of freedom. For example, the chirality couples to the magnetic field $\boldsymbol{h} = (h_x, h_y, h_z)$ as

$$F_h = -g_h h_z (h_y^3 - 3h_y h_x^2) \bar{\mathcal{C}}, \quad (4)$$

where g_h is a coupling constant. This coupling can be understood as follows. The chirality $\mathcal{C}$ is given by Eq. (1): $\mathcal{C} = \hat{Q}_x Q_{yz} - \hat{Q}_y Q_{zx}$. Here, the electric dipole operators $(\hat{Q}_x, \hat{Q}_y)$ in the sublattice degrees of freedom can be exactly rewritten in terms of the electric quadrupoles $(\hat{Q}_{x^2-y^2}, -\hat{Q}_{2xy})$, where $\hat{Q}_{\mu\nu} \equiv \sum_{n=1}^3 (\hat{\boldsymbol{r}}_n)_\mu (\hat{\boldsymbol{r}}_n)_\nu \hat{P}_n$, $\hat{Q}_{x^2-y^2} = \hat{Q}_{xx} - \hat{Q}_{yy}$, and $\hat{Q}_{2xy} = 2\hat{Q}_{xy}$. This formulation explicitly demonstrates that the chirality $\mathcal{C}$ transforms as the electric hexadecapole moment $Q_{z(y^3-3yx^2)}$:

$$\mathcal{C} = \hat{Q}_{x^2-y^2} Q_{yz} + \hat{Q}_{2xy} Q_{zx} \equiv Q_{z(y^3-3yx^2)}. \quad (5)$$

Thus, $\mathcal{C}$ can couple to the magnetic field as described in Eq. (4). The linear coupling F_h indicates that the conjugate field $h_z(h_y^3 - 3h_y h_x^2)$ can control the domain of chirality $\bar{\mathcal{C}}$, hardly achievable for the structural chirality of crystals.

Since $\mathcal{C}$ originates from the electric quadrupole $Q_{yz,xz}$ of localized electrons, it couples with the magnetic dipole moment $\boldsymbol{M} = (M_x, M_y, M_z)$ as

$$F_{\text{hyb}} = -g_{\text{hyb}} (\bar{Q}_{zx} \bar{M}_x + \bar{Q}_{yz} \bar{M}_y) \bar{M}_z = -g_{\text{hyb}} \bar{\mathcal{C}} \bar{\mathcal{T}} \bar{M}_z, \quad (6)$$

where $g_{\rm hyb}$ is a coupling constant, $\bar{\boldsymbol{M}} = \langle \boldsymbol{M} \rangle$, and $\bar{Q}_{yz(zx)} = \langle Q_{yz(zx)} \rangle$. Here, we define the magnetic toroidal dipole moment $\bar{\mathcal{T}} \equiv \langle \hat{Q}_x M_y - \hat{Q}_y M_x \rangle$. As a result, magnetic field $\boldsymbol{h} \parallel \boldsymbol{z}$ induces a noncoplanar magnetic configuration involving the magnetic toroidal dipole moment. The schematic illustration of the resulting magnetic moment configuration is shown in Fig. 2(d). $\bar{\mathcal{T}}$ induces several intriguing phenomena, such as the transverse magnetoelectric (ME) effect, characterized by $\alpha_{xy} = -\alpha_{yz} \neq 0$, and nonreciprocal transport (NRT) along the z-axis. Notably, the transverse ME effect contrasts with the longitudinal response $\alpha_{xx} = \alpha_{yy}$ induced by the chirality order. Furthermore, such a noncoplanar magnetic configuration can generate a large anomalous Hall effect due to the presence of finite scalar spin chirality.

Candidate: URhSn—We now discuss URhSn as an example of systems exhibiting the PEC order. In URhSn, the U sites form a distorted kagome structure [Fig. 1(b)]. This compound shows a ferromagnetic (FM) transition with the z-axis magnetization at $T_c = 16$ K, similar to other U-based isostructural compounds [24,27,38–40], and a second-order phase transition at $T_o = 54$ K [23–29]. The results of Mössbauer effect [27] and NMR [41] measurements suggest that this is a nonmagnetic transition. Since the entropy estimated at $T \simeq T_o = 54$ K is approximately $R \ln 3$, where R is the gas constant [28], the phase transition can be modeled by the localized f-electrons. We propose that the chiral order of the f-electrons' quadrupole moments is realized below T_o in URhSn, which is consistent with various experimental data. (i) The increasing transition temperature under $\boldsymbol{h} \parallel \boldsymbol{z}$, the negative Curie-Weiss temperature for the in-plane magnetic susceptibility [28], and the softening of the C_{66} elastic constant accompanied by its negative Curie-Weiss temperature [42] are all consistent with the antiferro (Q_{yz}, Q_{zx})-type quadrupole orders. (ii) The threefold symmetry in the thermal expansion measurement [28] suggests 120° orders. (iii) The canted magnetic moments in the FM phase [43], the NMR measurement [41,44,45], the early neutron scattering [26], and the recent resonant x-ray scattering [43] experiments all support the $\boldsymbol{q} = \boldsymbol{0}$ order of chirality $\mathcal{C}$. Specifically, the resonant x-ray scattering study has revealed that the possible ordered states in URhSn are restricted to either chiral or polar ones with $\boldsymbol{q} = \boldsymbol{0}$ [43], while an NMR study [41] and a polarized neutron scattering experiment [46] in preparation indicate that the ordered state is chiral rather than polar. As for the crystal structure, no structural distortion or atomic displacement has been detected within the experimental and analytical precision [26], indicating that the lattice remains essentially achiral even in the ordered phase. These facts strongly indicate that the order parameter below T_o is the electronic chirality discussed in this Letter. A mean-field analysis of a minimal localized model for URhSn is also presented in the SM [16]. It is noteworthy not only that URhSn realizes an electronic chirality order but also that the ferromagnetic order below T_c is accompanied by the emergence of a magnetic toroidal dipole $\bar{\mathcal{T}}$ due to the coupling $F_{\rm hyb}$ [Eq. (6)]. The temperature-field dependences of $\bar{\mathcal{T}}$-related phenomena, such as the ME effect, NRT, and the anomalous Hall effect, are particularly intriguing due to the presence of crossover effects from the ferromagnetic phase with $\bar{\mathcal{T}}$ at zero field to the chiral phase at finite magnetic field $\boldsymbol{h} \parallel \boldsymbol{z}$. These crossover effects manifest in various observables, providing further evidence of the chirality order.

At present, URhSn remains the only well-established candidate for PEC. This scarcity reflects the rarity of Q_{zx}/Q_{yz}-type quadrupole orders, which are uncommon in known materials. Nevertheless, several U-, Dy-, and Tb-based compounds have recently been reported to host such quadrupole orders, often in close connection with noncoplanar magnetic structures, in a manner reminiscent of URhSn [47–52]. These developments suggest that Q_{zx}/Q_{yz}-type orders are likely more widespread than currently recognized, and that additional cases will be identified. Consequently, the list of potential PEC candidate materials is expected to grow in the near future.

Discussion—We have introduced the concept of PEC, which originates from the internal degrees of freedom of electrons. Here, we discuss the characteristics of PEC in comparison with chirality as studied in previous works. One of the earliest measures of chirality is Lipkin's Zilch [53], $\boldsymbol{E} \cdot (\boldsymbol{\nabla} \times \boldsymbol{E}) + \boldsymbol{B} \cdot (\boldsymbol{\nabla} \times \boldsymbol{B})$, which represents the chirality of electromagnetic fields. In chiral crystals or molecules, the structural chirality gives rise to finite $\boldsymbol{E} \cdot (\boldsymbol{\nabla} \times \boldsymbol{E})$, and the electronic chirality $\boldsymbol{p} \cdot \boldsymbol{\sigma}$, where $\boldsymbol{p}$ is the momentum of electrons, becomes finite in the bulk through the spin-orbit coupling $\propto \boldsymbol{E} \cdot (\boldsymbol{p} \times \boldsymbol{\sigma})$ [13,14]. In magnetically ordered crystals, magnetic structural chirality generates $\boldsymbol{B} \cdot (\boldsymbol{\nabla} \times \boldsymbol{B})$, leading to, e.g., a spin-momentum locking of the form $\boldsymbol{k} \cdot \boldsymbol{\sigma}$ in helimagnets [54]. In contrast, the PEC introduced in this Letter is neither induced by $\boldsymbol{E} \cdot (\boldsymbol{\nabla} \times \boldsymbol{E})$ nor $\boldsymbol{B} \cdot (\boldsymbol{\nabla} \times \boldsymbol{B})$, but it emerges under the electronic ordering via Eq. (1) $\sim \boldsymbol{r} \cdot (\boldsymbol{l} \times \boldsymbol{\sigma})$. Here, $\boldsymbol{r}$ is the electrons' position. The form $\boldsymbol{r} \cdot (\boldsymbol{l} \times \boldsymbol{\sigma})$ indeed appears in the exact quantum mechanical operator expression of $\boldsymbol{p} \cdot \boldsymbol{\sigma}$ [55].

While structural chirality induces electronic chirality, the reverse is not necessarily true. In candidate PEC systems, no irreducible mode of lattice displacement transforms as G_0. With regard to dynamical chirality of lattices, however, the PEC can affect phonons, generating truly chiral phonons [1,56,57]. In the case of the distorted kagome lattice, the chirality-related term $\propto \bar{\mathcal{C}}(\hat{Q}_x\{L_y, L_z\} - \hat{Q}_y\{L_z, L_x\})$ similar to Eq. (1) emerges in the dynamical matrix due to electron-phonon couplings, where $\boldsymbol{L}$ represents angular momentum of phonons. Here, $\{L_{y(x)}, L_z\}$ reflects the anisotropic charge distribution associated with

the quadrupole order, arising from the conventional Coulomb interaction between electrons and nuclei. The dynamical matrix also includes the term $\propto (k_x\hat{Q}_y - k_y\hat{Q}_x)L_z$, which is similar to Eq. (3) and independent of electron-phonon couplings. The presence of these two terms leads to the momentum-angular momentum coupling $\propto \bar{C}(k_xL_x + k_yL_y)$ in the optical modes, which gives rise to the truly chiral phonons. Its magnitude is estimated to be on the order of a few percent of the ordinary phonon energy scale, as discussed in the SM [16]. The emergence of truly chiral phonons in an achiral crystal serves as an analog of PEC and occurs exclusively in PEC systems.

From the perspective of chirality manipulation, controlling the domain of chirality order has been achieved only via the control of simultaneously emerging ferroelectric and ferroelastic order parameters [58–64]. In contrast, the domain control in our model can be achieved by magnetic field via the electric hexadecapole $Q_{z(y^3-3yx^2)}$ coupled to $h_z(h_y^3 - 3h_yh_x^2)$. Because such chirality switching does not involve any lattice displacements, it is expected to occur on timescales much faster than those in structurally chiral systems. Magnetic-field-induced domain control of an electric quadrupole order was recently demonstrated [65]. This suggests that domains of electronic chirality originating from electric quadrupoles should likewise be controllable by magnetic fields. For the candidate compound URhSn, the enantiomer separation can be observed by the Sn-NMR measurement under the magnetic field in the yz plane [41,44]. Regarding the lattice displacements in the chiral phase of URhSn, the Rh ions at the $2d$ Wyckoff position of space group $P\bar{6}2m$ may move along the z direction, while the U ions at the distorted kagome sites remain stationary. Thus, the chirality order in URhSn is not purely electronic but a composite one with the structural chirality, although no atomic displacement has been detected experimentally. If such atomic displacements are present, they could indicate sufficiently strong electron-lattice coupling, opening a pathway to controlling structural chirality through magnetic fields via their coupling to the electronic chirality. As a consequence of such chirality control, the Flack parameter in x-ray diffraction [66], which reflects the domain volume ratio of structural chirality, can be tuned to 0 or 1 by magnetic fields in the yz plane, which is hardly achievable in chiral crystals or chiral ferroelectrics.

Summary—We have introduced the concept of nonstructural, purely electronic chirality. As a representative example, we consider an electric quadrupole order with a 120° structure on a distorted kagome lattice. This system exhibits a $\boldsymbol{k}\cdot\boldsymbol{\sigma}$-type spin-momentum locking despite the absence of structural chirality. To explore potential realizations in real materials, we analyze the chirality order in URhSn and demonstrate the possibility of manipulating the chiral domain via magnetic fields. Furthermore, couplings between PEC and lattices give rise to truly chiral phonons in achiral crystals, which represent a phonon analog of PEC. The concept of purely electronic chirality opens up an avenue for distinguishing the origins of chirality, which will contribute to a deeper understanding of its underlying principles and application development.

Acknowledgments—The authors thank C. Tabata, Y. Tokunaga, Y. Shimizu, T. Yanagisawa, and H. Kusunose for fruitful discussions. This work was supported by JSPS KAKENHI (Grants No. JP21H01031, No. JP23H04866, No. JP23H04869, No. JP23K20824) from the Japan Society for the Promotion of Science.

Data availability—The data are not publicly available. The data are available from the authors upon reasonable request.

[1] L. D. Barron, Chirality **24**, 879 (2012).
[2] L. Pasteur, Ann. Chim. **24**, 442 (1848).
[3] T. D. Lee and C. N. Yang, Phys. Rev. **104**, 254 (1956).
[4] C. S. Wu, E. Ambler, R. W. Hayward, D. D. Hoppes, and R. P. Hudson, Phys. Rev. **105**, 1413 (1957).
[5] J. D. Watson and F. H. Crick, Nature (London) **171**, 737 (1953).
[6] L. D. Barron, Space Sci. Rev. **135**, 187 (2008).
[7] R. Oiwa and H. Kusunose, Phys. Rev. Lett. **129**, 116401 (2022).
[8] J.-I. Kishine, H. Kusunose, and H. M. Yamamoto, Isr. J. Chem. **62**, 202200049 (2022).
[9] S. Hayami and H. Kusunose, J. Phys. Soc. Jpn. **87**, 033709 (2018).
[10] H. Kusunose, R. Oiwa, and S. Hayami, J. Phys. Soc. Jpn. **89**, 104704 (2020).
[11] S. Hoshino, M.-T. Suzuki, and H. Ikeda, Phys. Rev. Lett. **130**, 256801 (2023).
[12] S. Hayami and H. Kusunose, J. Phys. Soc. Jpn. **92**, 113704 (2023).
[13] T. Miki, M.-T. Suzuki, H. Ikeda, and S. Hoshino, Phys. Rev. Lett. **134**, 226401 (2025).
[14] A. Inda, R. Oiwa, S. Hayami, H. M. Yamamoto, and H. Kusunose, J. Chem. Phys. **160**, 184117 (2024).
[15] S. Hayami, M. Yatsushiro, Y. Yanagi, and H. Kusunose, Phys. Rev. B **98**, 165110 (2018).
[16] See Supplemental Material at http://link.aps.org/supplemental/10.1103/dc1q-xzbd, which includes Refs. [17–22] and provides a detailed description of the conduction electron model, an extended analysis of the microscopic origin of spin-momentum locking, results from mean-field analyses of a microscopic localized model for URhSn, additional examples of PEC orders in other systems, and a quantitative estimation of the chiral phonon term.
[17] T. Ishitobi and K. Hattori, J. Phys. Soc. Jpn. **88**, 063708 (2019).
[18] M. T. Hutchings, Solid State Phys. **16**, 227 (1964).
[19] R. Shiina, H. Shiba, and P. Thalmeier, J. Phys. Soc. Jpn. **66**, 1741 (1997).
[20] A. J. Freeman and R. E. Watson, Phys. Rev. **127**, 2058 (1962).

[21] P. Santini, S. Carretta, G. Amoretti, R. Caciuffo, N. Magnani, and G. H. Lander, Rev. Mod. Phys. **81**, 807 (2009).

[22] K. Ishito, H. Mao, K. Kobayashi, Y. Kousaka, Y. Togawa, H. Kusunose, J.-I. Kishine, and T. Satoh, Chirality **35**, 338 (2023).

[23] T. T. M. Palstra, G. J. Nieuwenhuys, R. F. M. Vlastuin, J. van den Berg, J. A. Mydosh, and K. H. J. Buschow, J. Magn. Magn. Mater. **67**, 331 (1987).

[24] V. H. Tran and R. Troć, J. Magn. Magn. Mater. **102**, 74 (1991).

[25] V. H. Tran, R. Troć, and D. Badurski, J. Alloys Compd. **219**, 285 (1995).

[26] F. Mirambet, B. Chevalier, L. Fournés, J. F. da Silva, M. Frey Ramos, and T. Roisnel, J. Magn. Magn. Mater. **140–144**, 1387 (1995).

[27] R. Kruk, R. Kmiec-acute, K. Łotka, K. Tomala, R. Troc-acute, and V. H. Tran, Phys. Rev. B **55**, 5851 (1997).

[28] Y. Shimizu, A. Miyake, A. Maurya, F. Honda, A. Nakamura, Y. J. Sato, D. Li, Y. Homma, M. Yokoyama, Y. Tokunaga, M. Tokunaga, and D. Aoki, Phys. Rev. B **102**, 134411 (2020).

[29] A. Maurya, D. Bhoi, F. Honda, Y. Shimizu, A. Nakamura, Y. J. Sato, D. Li, Y. Homma, M. Sathiskumar, J. Gouchi, Y. Uwatoko, and D. Aoki, Phys. Rev. B **104**, 195119 (2021).

[30] H. Kusunose, R. Oiwa, and S. Hayami, Phys. Rev. B **107**, 195118 (2023).

[31] S. Hayami, Y. Yanagi, and H. Kusunose, Phys. Rev. B **101**, 220403(R) (2020).

[32] R. Oiwa and H. Kusunose, J. Phys. Soc. Jpn. **91**, 014701 (2022).

[33] S. Hayami and H. Kusunose, J. Phys. Soc. Jpn. **93**, 072001 (2024).

[34] S. R. Park, C. H. Kim, J. Yu, J. H. Han, and C. Kim, Phys. Rev. Lett. **107**, 156803 (2011).

[35] S. S. Brinkman, X. L. Tan, B. Brekke, A. C. Mathisen, O. Finnseth, R. J. Schenk, K. Hagiwara, M.-J. Huang, J. Buck, M. Kalläne, M. Hoesch, K. Rossnagel, K.-H. Ou Yang, M.-T. Lin, G.-J. Shu, Y.-J. Chen, C. Tusche, and H. Bentmann, Phys. Rev. Lett. **132**, 196402 (2024).

[36] V. Edelstein, Solid State Commun. **73**, 233 (1990).

[37] G. Furuya and K. Hattori, Phys. Rev. B **112**, 035171 (2025).

[38] V. Sechovsky, L. Havela, F. R. De Boer, J. J. M. Franse, P. A. Veenhuizen, J. Sebek, J. Stehno, and A. V. Andreev, Physica (Amsterdam) **142B+ C**, 283 (1986).

[39] N. V. Mushnikov, T. Goto, K. Kamishima, H. Yamada, A. V. Andreev, Y. Shiokawa, A. Iwao, and V. Sechovsky, Phys. Rev. B **59**, 6877 (1999).

[40] D. Aoki, T. Combier, V. Taufour, T. D. Matsuda, G. Knebel, H. Kotegawa, and J. Flouquet, J. Phys. Soc. Jpn. **80**, 094711 (2011).

[41] Y. Tokunaga *et al.* (unpublished).

[42] T. Yanagisawa *et al.* (unpublished).

[43] C. Tabata, F. Kon, R. Hibino, Y. Shimizu, H. Amitsuka, K. Kaneko, Y. Homma, D. Aoki, and H. Nakao, J. Phys. Soc. Jpn. **94**, 083701 (2025).

[44] H. Kusunose and J. Kikuchi, J. Phys. Soc. Jpn. **93**, 074701 (2024).

[45] H. Harima, SciPost Phys. Proc. **11**, 006 (2023).

[46] C. Tabata *et al.* (unpublished).

[47] R. Watanuki, G. Sato, K. Suzuki, M. Ishihara, T. Yanagisawa, Y. Nemoto, and T. Goto, J. Phys. Soc. Jpn. **74**, 2169 (2005).

[48] K. A. McEwen, H. C. Walker, Le, D. F. McMorrow, E. Colineau, F. Wastin, S. B. Wilkins, J.-G. Park, R. I. Bewley, and D. Fort, J. Magn. Magn. Mater. **310**, 718 (2007).

[49] N. Sanada, T. Muneoka, R. Watanuki, K. Suzuki, M. Akatsu, and T. Sakakibara, J. Phys. Conf. Ser. **150**, 042172 (2009).

[50] T. Shigeoka, T. Fujiwara, K. Munakata, K. Matsubayashi, and Y. Uwatoko, J. Phys. Conf. Ser. **273**, 012127 (2011).

[51] I. Ishii, T. Mizuno, K. Takezawa, S. Kumano, Y. Kawamoto, T. Suzuki, D. I. Gorbunov, M. S. Henriques, and A. V. Andreev, Phys. Rev. B **97**, 235130 (2018).

[52] T. Kurumaji, M. Gen, S. Kitou, K. Ikeuchi, H. Sagayama, H. Nakao, T. R. Yokoo, and T.-H. Arima, Nat. Commun. **16**, 2176 (2025).

[53] D. M. Lipkin, J. Math. Phys. **5**, 696 (1964).

[54] B. Brekke, P. Sukhachov, H. G. Giil, A. Brataas, and J. Linder, Phys. Rev. Lett. **133**, 236703 (2024).

[55] H. Kusunose, J.-I. Kishine, and H. M. Yamamoto, Appl. Phys. Lett. **124**, 260501 (2024).

[56] J. Kishine, A. S. Ovchinnikov, and A. A. Tereshchenko, Phys. Rev. Lett. **125**, 245302 (2020).

[57] K. Ishito, H. Mao, Y. Kousaka, Y. Togawa, S. Iwasaki, T. Zhang, S. Murakami, J.-I. Kishine, and T. Satoh, Nat. Phys. **19**, 35 (2022).

[58] H. Iwasaki and K. Sugii, Appl. Phys. Lett. **19**, 92 (1971).

[59] H. Iwasaki, K. Sugii, N. Niizeki, and H. Toyoda, Ferroelectrics **3**, 157 (1972).

[60] J. Kobayashi, K. Uchino, H. Matsuyama, and K. Saito, J. Appl. Phys. **69**, 409 (1991).

[61] D. D. Khalyavin, R. D. Johnson, F. Orlandi, P. G. Radaelli, P. Manuel, and A. A. Belik, Science **369**, 680 (2020).

[62] A. Sawada, Y. Ishibashi, and Y. Takagi, J. Phys. Soc. Jpn. **43**, 195 (1977).

[63] T. Hayashida, K. Kimura, D. Urushihara, T. Asaka, and T. Kimura, J. Am. Chem. Soc. **143**, 3638 (2021).

[64] Z. Zeng, M. Först, M. Fechner, M. Buzzi, E. B. Amuah, C. Putzke, P. J. W. Moll, D. Prabhakaran, P. G. Radaelli, and A. Cavalleri, Science **387**, 431 (2025).

[65] M. Manago, A. Ishigaki, H. Tou, H. Harima, H. Tanida, and H. Kotegawa, Phys. Rev. B **108**, 085118 (2023).

[66] H. D. Flack, Acta Crystallogr. Sect. A **39**, 876 (1983).